

设计指南: TIDA-01292

适用于低频离线 UPS 和逆变器且不带散热器的 650W 功率级参考设计



说明

此参考设计是一款专为低频（基于变压器）单相 UPS（由 12V 电池供电）设计的 650W 逆变器功率级。

此设计凭借采用 SON5x6 封装且具有极低 $R_{DS(ON)}$ 和低栅极电荷 (Q_g) 的 TI SMD MOSFET，实现小外形尺寸和高效率的解决方案。通过在全桥功率级的每个桥臂上并联使用两个器件，该功率级消除了散热器需求，从而降低了总体系统成本。

为了驱动 MOSFET，此设计采用了 LM5101B，这是一个具有高压摆率的 2A 栅极驱动器，可进一步降低开关损耗。此设计采用双向电流感应放大器 INA181 来进行精密电流感应，从而实现过流和短路保护。此设计通过 TI Piccolo™ 微控制器 TMS320F28027 LaunchPad™ 实现了可提供高频正弦 PWM 运行模式和强大保护功能的固件。

该电路板在电阻和电感负载条件下都经过了与低频变压器（12V 交流电：220V 交流电）配合使用的测试。此外，该电路板还经验证具有运行稳定性以及内置的欠压、过压、过载和短路保护功能。

资源

[TIDA-01292](#)

[CSD17573Q5B](#)

[LM5101B](#)

[INA181](#)

[TLV704](#)

[LMV431B](#)

[LMT88](#)

设计文件夹
产品文件夹
产品文件夹
产品文件夹
产品文件夹
产品文件夹
产品文件夹



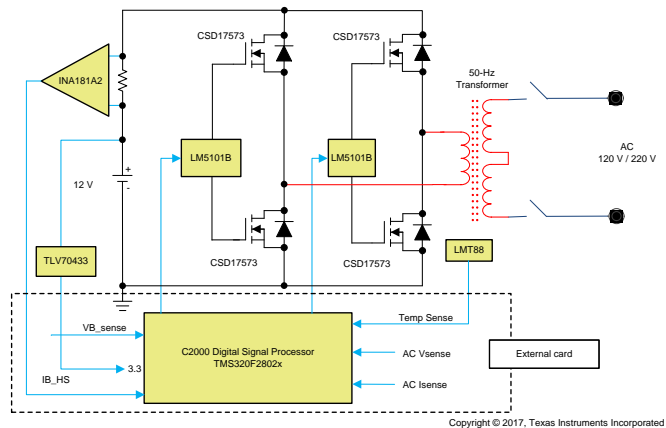
咨询我们的 E2E 专家

特性

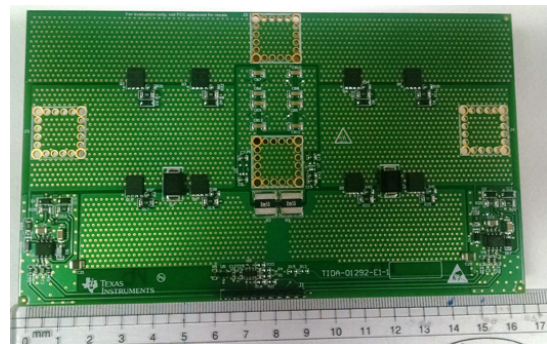
- 专为 100VA 至 850VA 的待机或离线 UPS 设计，可通过并联更多 FET 扩展到 1.5kVA
- 采用 SMD MOSFET 的解决方案提高了 UPS 的可制造性和组装性
- 无需功耗散热器，因此降低了系统成本并缩短生产时间
- 经过测试和验证，在采用灯泡负载时的工作功率达 100W 至 650W
- 典型效率约为 95%，最大效率大于 98.5%
- 过流、短路、过压和欠压保护

应用

- 离线和待机 UPS
- 直流转交流逆变器
- 能量存储系统
- 家用和住宅逆变器



Copyright © 2017, Texas Instruments Incorporated





该 TI 参考设计末尾的重要声明表述了授权使用、知识产权问题和其他重要的免责声明和信息。

1 System Description

A power inverter is a device that converts electrical power from a DC form to an AC form using electronic circuits. Its typical application is to convert battery voltage into conventional household AC voltage, allowing one to use household electronic equipment when AC power is not available. There are three kinds of inverters. The first set of inverters made produced a square wave signal at the output as shown in 图 1; however, these are now obsolete.

The modified-square wave, also known as the modified-sine wave inverter, produces square waves with some dead spots between positive and negative half-cycles at the output. The cleanest utility supply-like power source is provided by a pure sine wave inverter. The present inverter market is going through a shift from traditional modified-sine wave inverters to pure sine wave inverters because of the benefits that these inverters offer.

These inverters are also part of energy storage systems where the charging of the battery is done through renewable energy means such as solar and wind, and DC-to-AC conversion is done through inverters.

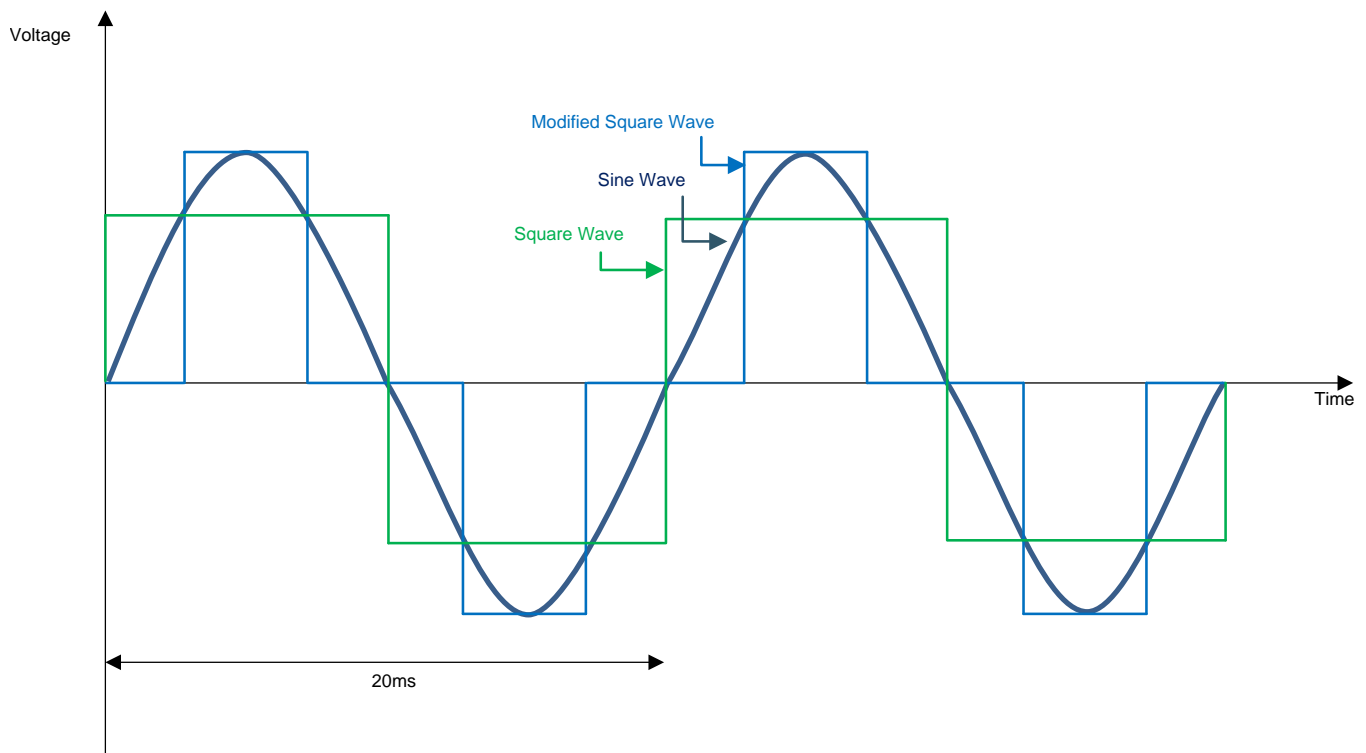
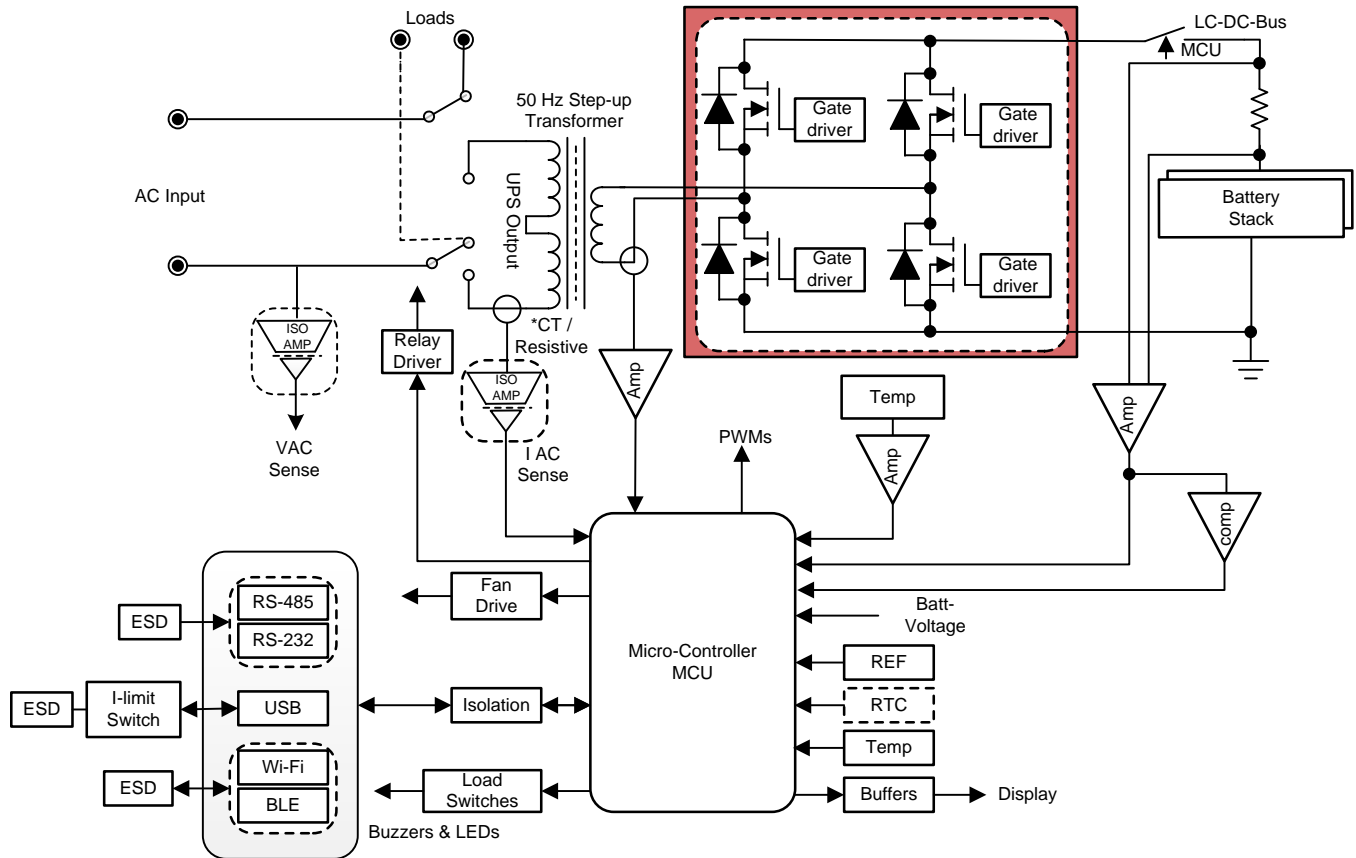


图 1. Types of Inverter Outputs

1.1 Design of Pure Sine Wave Inverter

图 2 shows the system block diagram of a single-phase UPS.



Copyright © 2017, Texas Instruments Incorporated

图 2. System Block Diagram of Single-Phase UPS

There are two modes of operation in a residential inverter: mains mode and inverter mode. An inverter not only converts the battery voltage to 220/120-V AC but also charges the battery when the AC mains is present.

The method in which the low-voltage DC power is converted to AC is generally done in two steps:

1. Convert low-voltage DC power to a high-voltage DC source.
2. Convert high-voltage DC to AC waveform using pulse width modulation (PWM). This step is also called a transformer-less approach.

Another method to achieve the desired outcome would be to first convert the low-voltage DC power to AC, then use a transformer to boost the voltage to 120 or 220 V (thus called the transformer-based inverter). This method is widely used in residential inverters, on which this reference design is based.

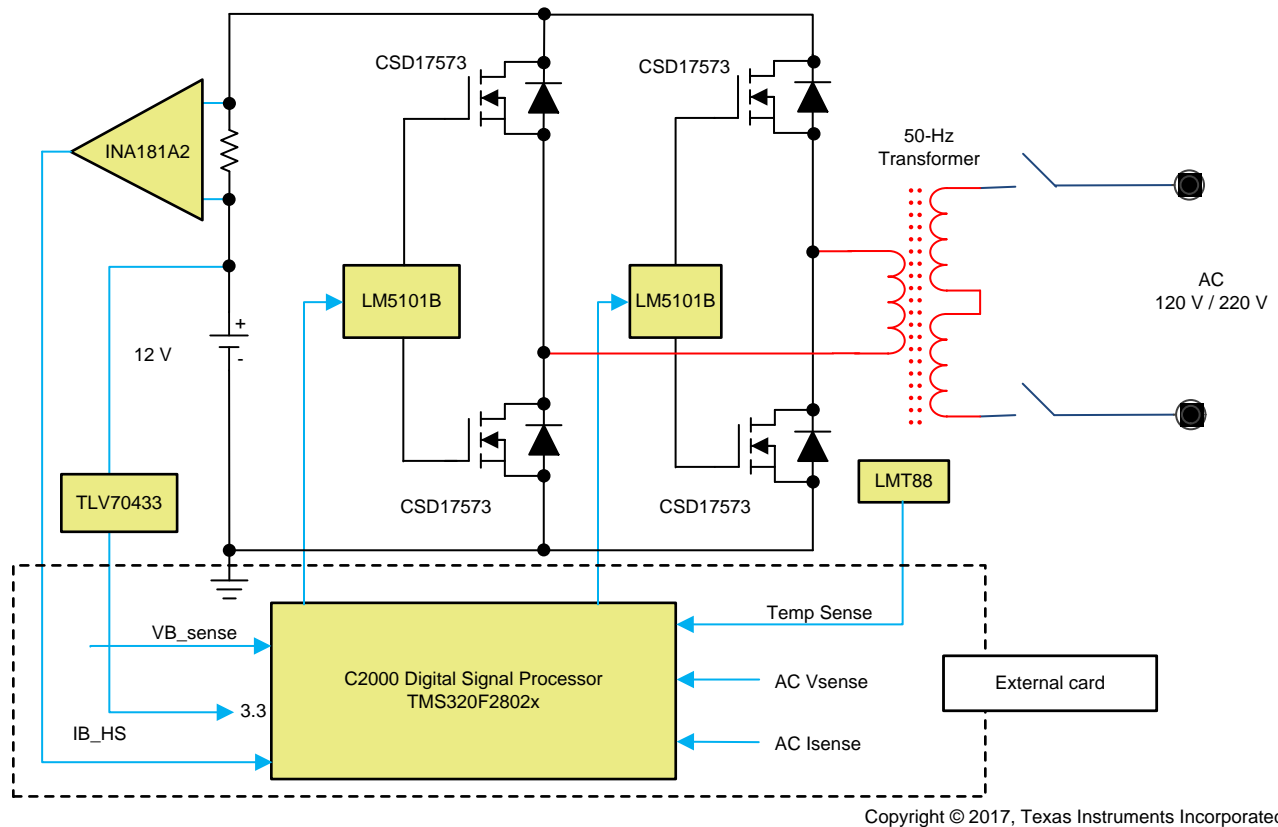
1.2 Key System Specifications

表 1. Key System Specifications

PARAMETER	MIN	TYP	MAX	UNIT
Input voltage	10	12	14	VDC
Rated output power	550	650	750	W
Switching frequency	—	12	—	kHz
Cooling	400	600	800	LFM
Operating ambient	-20	25	55	°C
Efficiency	—	95	98.6	%
Protections	Overcurrent			
	Overvoltage			
	Undervoltage			
	Overtemperature			
Board specification	90 mm x 155 mm, two-layer, 2-oz copper			

2 System Overview

2.1 Block Diagram



2.2 Highlighted Products

2.2.1 CSD17573Q5B

This design uses eight CSD17573Q5B MOSFETs to form the inverter stage. This FET was chosen due to its low $R_{DS(on)}$ of $0.84m\Omega$ and a low-gate charge, designed to minimize the losses in power conversion and switching applications. The device comes in a compact, 8-pin SON 5-mm \times 6-mm package.

Key features of the CSD17573Q5B include:

- Low Q_g and Q_{gd}
- Ultra-low $R_{DS(on)}$
- Low-thermal resistance
- Avalanche rated
- Lead-free terminal plating
- RoHS compliant
- Halogen free
- SON 5-mm \times 6-mm plastic package

2.2.2 LM5101B

This design uses two LM5101B devices. The LM5101B high-voltage gate driver is designed to drive both the high- and the low-side N-channel MOSFETs in a synchronous buck or a half-bridge configuration. The floating high-side driver is capable of operating with supply voltages up to 100 V. The LM5101B provides 2 A of gate drive. The outputs are independently controlled with CMOS input thresholds.

An integrated high-voltage diode is provided to charge the high-side gate drive bootstrap capacitor. A robust level shifter operated at high speed while consuming low power and providing clean level transitions from the control logic to the high-side gate driver. Undervoltage lockout is provided on both the low-side and the high-side power rails.

Key features of the LM5101B include:

- Drives both a high- and low-side N-channel MOSFETs
- Independent high-and low-driver logic inputs
- Bootstrap supply voltage up to 118-V DC
- Fast propagation times: 25 ns typical
- Drives 1000-pF load with 8-ns rise and fall time
- Excellent propagation delay matching: 3 ns typical
- Supply rail undervoltage lockout
- Low power consumption

2.2.3 INA181

This design uses the INA181 to sense the current through MOSFETs and to protect the system for overcurrent. The INA181 device is a bidirectional current sense amplifier that senses voltage drop across current sense resistors at common-mode voltages from -0.2 to 26V, independent of the supply voltage. This design uses the A2 version with fixed gain of 50, which is achieved by integrated matched resistor gain network to minimize the gain error and reduce the temperature drift.

Key features of the INA181 include:

- Common-mode range (V_{CM}): -0.2 to 26 V
- High bandwidth: 350 kHz
- Offset voltage:
 - ± 150 μ V (max) at $V_{CM} = 0$ V
 - ± 500 μ V (max) at $V_{CM} = 12$ V
- Output slew rate: 2 V/ μ s
- Bidirectional current-sensing capability
- Accuracy:
 - $\pm 1\%$ gain error (max)
 - 1- μ V/ $^{\circ}$ C offset drift (max)
- Gain Options:
 - 20 V/V (A1 devices)
 - 50 V/V (A2 devices)
 - 100 V/V (A3 devices)

- 200 V/V (A4 devices)
- Quiescent current: 260 μ A (max per channel)

2.2.3.1 INA185

For higher-performance current sensing and overcurrent protection, the INA185 current sense amplifier can be considered.

Benefits of the INA185 over the INA181 include:

- Offset voltage:
 - $\pm 55 \mu\text{V}$ (max) at $V_{\text{CM}} = 0 \text{ V}$ (A2 device)
 - $\pm 130 \mu\text{V}$ (max) at $V_{\text{CM}} = 12 \text{ V}$ (A2 device)
- Accuracy:
 - $\pm 0.2\%$ gain error (max, A2 device)
 - $0.5 \mu\text{V}/^\circ\text{C}$ offset drift (max)
- Small package:
 - SOT-563 (6): $1.6\text{mm} \times 1.6\text{mm}$ (including pins)

2.3 System Design Theory

2.3.1 Inverter Operation and PWM Explanation

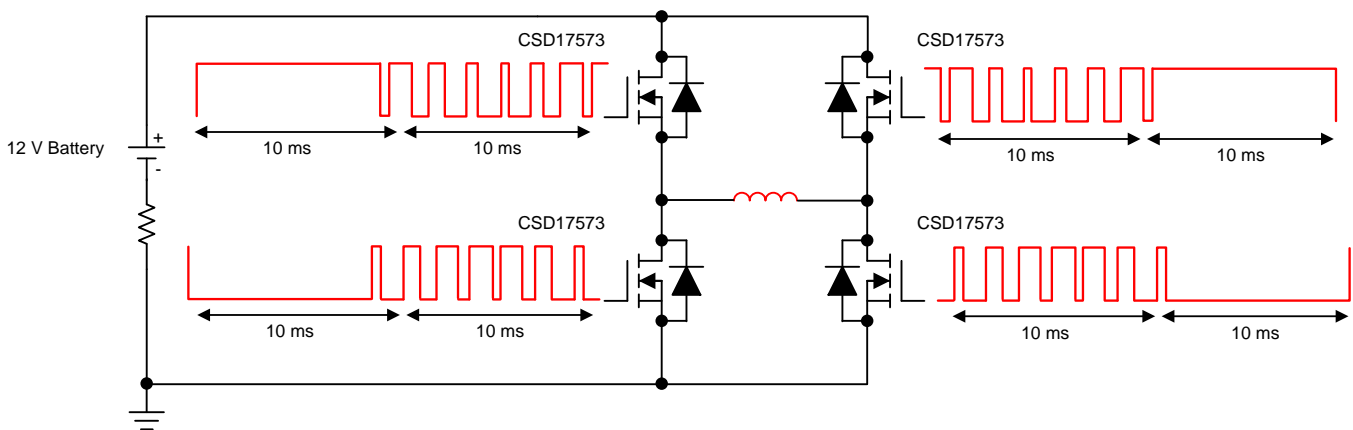
The DC-to-AC inversion can be achieved using two methods:

1. The first is the conversion of low-voltage DC to a high-voltage DC followed by the conversion of this high-voltage DC to AC using PWM.
2. Another method is to first convert the low-voltage DC to AC and then use a transformer to boost the voltage to 120 or 220 V.

This design uses the second method of inverting DC to AC using an H-bridge circuit where the MOSFETs are switched with high frequency SPWM signals. The switching waveforms used for this design is explained in the following subsections.

2.3.1.1 Switching Waveforms

图 3 shows the sine PWM used for each switch:



Copyright © 2017, Texas Instruments Incorporated

图 3. SPWM Sequence Used for TIDA-01292

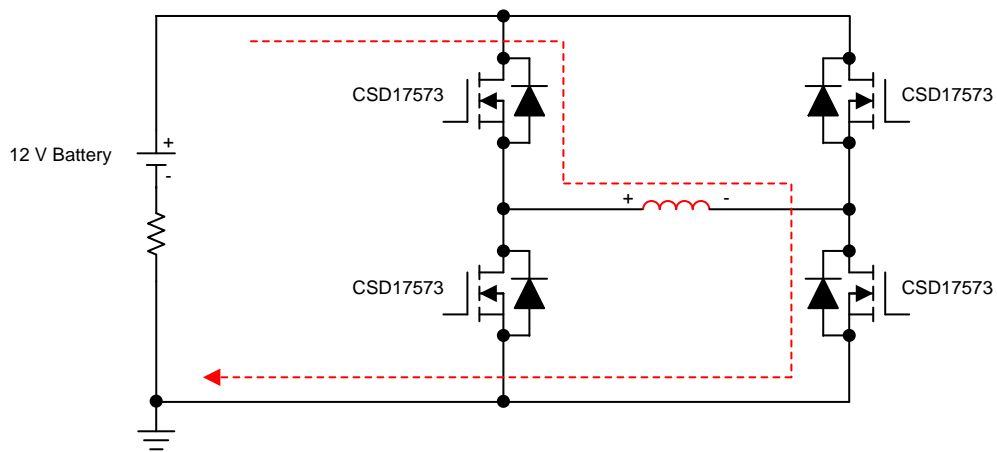
The switching algorithm as shown in 图 3 can be broken in following sequence:

1. The 50-Hz sine output can be divided into two time intervals of 10 ms each.
2. During the first 10 ms:
 - The left leg is switched at 50 Hz (that is, the top-left FET) is continuously on for 10 ms and the bottom-left FET is continuously off for that time.
 - The top- and bottom-right FETs are switched at a high frequency (12 kHz in this case) such that the duty cycle for the bottom FET goes from 0 to maximum and back to 0 while the duty cycle of the top FET varies from maximum to 0 and back to maximum in sinusoidal modulation.
3. During the next 10 ms:
 - The right leg is switched at 50 Hz (that is, the top-right FET) is continuously on for 10 ms and bottom-right FET is continuously off for the same 10ms period.
 - The top- and bottom-left FETs are switched at a high frequency (12 kHz in this case) such that the duty cycle for the bottom FET goes from 0 to maximum and back to 0 while the duty cycle of the top FET varies from maximum to 0 and back to maximum in sinusoidal modulation.

2.3.1.2 Power Flow

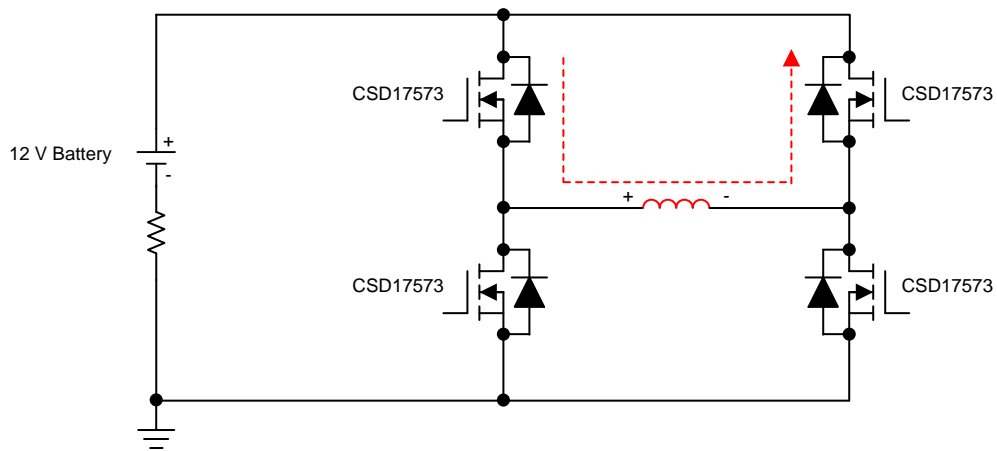
图 4 到 图 7 显示整个 50-Hz 周期的功率流。

图 4 显示了在正半周期期间从输入到输出的功率转移，如之前提到的，顶部左侧 FET 保持开启且底部左侧 FET 保持关闭连续 10 ms，而右侧 FET 以高频 SPWM 进行切换。如图 5 所示，在正半周期期间，电流通过顶部右侧 FET 的体二极管进行续流，直到 FET 被切换开启。这确保了设计在顶部 FET 上实现 ZVS 切换。



Copyright © 2017, Texas Instruments Incorporated

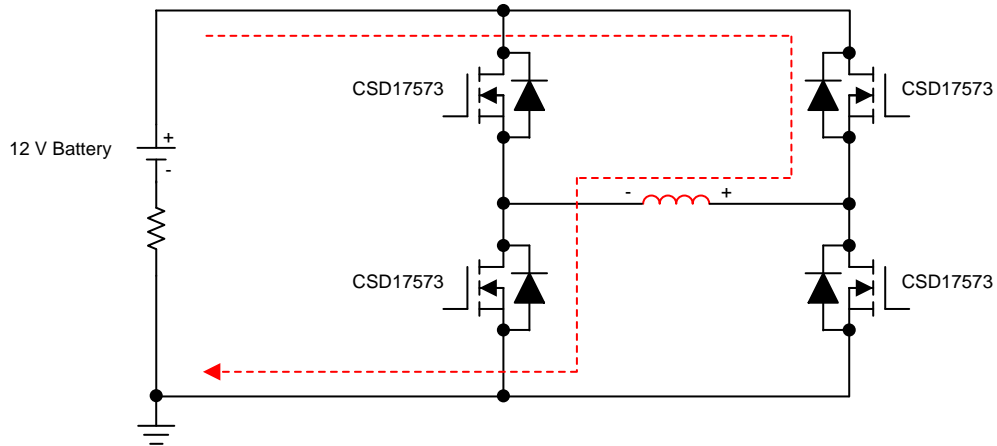
图 4. Increasing Positive Output



Copyright © 2017, Texas Instruments Incorporated

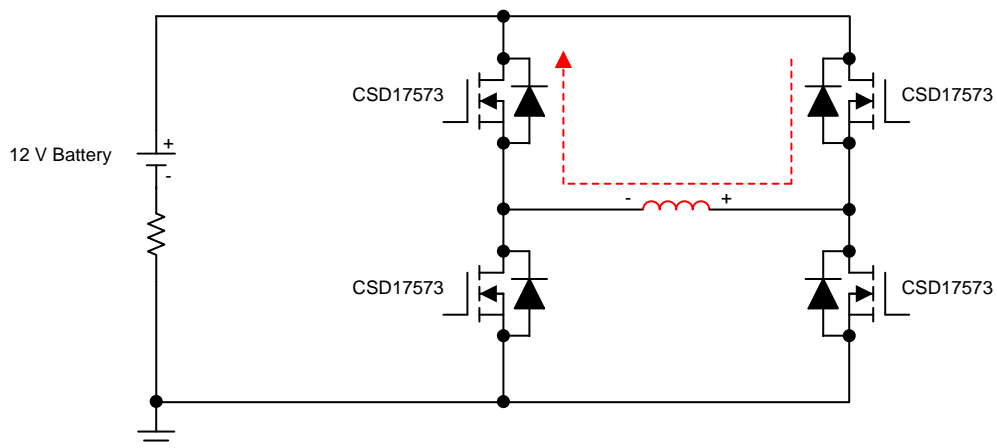
图 5. Decreasing Positive Output

A similar power flow sequence takes place in the negative half cycle where the top-right FET is continuously on and the bottom-right FET is continuously off while the left leg is switched. As a result, the power flow takes place when the left bottom FET is on and freewheeling happens when the left top FET is on, as shown in 图 6 and 图 7.



Copyright © 2017, Texas Instruments Incorporated

图 6. Increasing Negative Output



Copyright © 2017, Texas Instruments Incorporated

图 7. Decreasing Negative Output

The positive peak of the sine wave is achieved during maximum duty cycle switching of the bottom-right FET, and the negative peak is observed when the bottom-left FET is switched at the highest duty cycle. Also, the top FETs are always synchronous switching, which reduces the switching loss across them, while the bottom FETs are kept off for half the cycle and only switched during the other half, which reduces the conduction losses across them.

2.3.2 Gate Driver Design

2.3.2.1 Bootstrap and VDD Capacitor

The bootstrap capacitor must maintain the HB pin voltage above the UVLO voltage for the HB circuit in any circumstances during normal operation. Thus, the maximum allowable drop across the bootstrap capacitor is calculated with lowest battery voltage, as shown in [公式 1](#):

$$\Delta V_{HB} = V_{DD} - V_{DH} - V_{HBL} = 10 - 0.7 - 6.7 = 2.6 \text{ V} \quad (1)$$

where:

- V_{DD} = Supply voltage of the gate drive IC
- V_{DH} = Bootstrap diode forward voltage drop
- $V_{HBL} = V_{HBR} - V_{HBH} = 6.7 \text{ V}$, HB falling threshold based on the [LM5101B datasheet](#) (SNOSAW2)

The maximum quiescent current required by the driver and the bootstrap circuit is 0.2 mA as per the LM5101B datasheet. Also, due to the kind of switching scheme implemented for the inverter, the top FET remains on for 10 ms continuously; thus, the bootstrap capacitor must be able to supply the charge required during this entire time. The total charge required by the bootstrap capacitor can be calculated using [公式 2](#):

$$Q_{\text{Total}} = Q_{g\text{max}} + I_{HB\text{max}} \times T_{\text{on}} \quad (2)$$

where:

- $Q_{g\text{max}}$ is the total gate charge of the FET
- $I_{HB\text{max}}$ is the maximum quiescent current requirement of the driver and the bootstrap circuit
- T_{on} is the maximum on time of the FET (10 ms)

The total charge required by the bootstrap capacitor is: $Q_{\text{Total}} = 64 \text{ nC} + 0.2 \text{ mA} \times 10 \text{ ms} = 2.064 \text{ }\mu\text{C}$

The value of the bootstrap capacitor is calculated using [公式 3](#):

$$C_{\text{BOOT}} = \frac{Q_{\text{Total}}}{\Delta V_{HB}} = \frac{2.064 \text{ }\mu\text{C}}{2.6 \text{ V}} = 0.8 \text{ }\mu\text{F} \quad (3)$$

In practice, the value for the C_{BOOT} capacitor must be greater than the calculated value to allow for situations where the power stage may skip a pulse due to load transients. It is recommended to use 10 times the calculated value and place the bootstrap capacitor as close to the HB and HS pin as possible. A 10- μF capacitor is used for C_{BOOT} in this design.

As a general rule, the local V_{DD} bypass capacitor must be 10 times greater than the value of C_{BOOT} . For this design, a 100- μF electrolytic capacitor and a 10- μF ceramic capacitor is used for the V_{DD} supply.

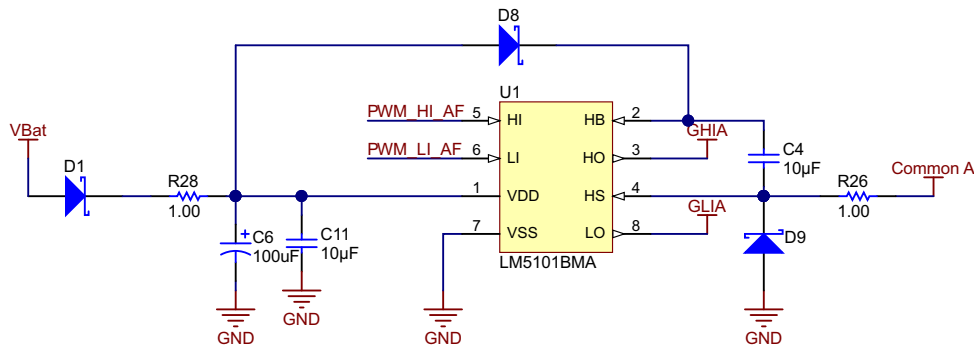
2.3.2.2 External Bootstrap Diode and Resistor

The bootstrap capacitor is charged by the V_{DD} through the internal bootstrap diode every cycle when the low-side MOSFET turns on. The charging of the capacitor involves high-peak currents; therefore, transient power dissipation in the internal bootstrap diode may be significant and dependent on its forward voltage drop. Both the diode conduction losses and reverse recovery losses contribute to the total losses in the gate driver and need to be considered in the power dissipation of the gate driver.

For high-frequency and high-capacitive loads, consider using an external bootstrap diode placed in parallel with the internal bootstrap diode to reduce power dissipation of the driver. For this design, a 20-V Schottky diode with a typical forward voltage drop of 0.38V at 1A is used in parallel to the internal bootstrap diode.

Bootstrap resistor R_{BOOT} is selected to reduce the inrush current in D_{BOOT} and limit the ramp-up slew rate of the voltage of HB-HS. This resistor serves two purposes: one is limiting the inrush current through D_{BOOT} ; the other is protecting the driver from the negative voltage spikes at the common-mode point. The value of this resistor must be just large enough to protect the diode. A very large value resistor cannot be used because this creates a potential difference between the source of the high-side MOSFET and the HS pin of the driver at the beginning of the PWM cycles until the C_{BOOT} is not charged to full voltage. Due to this potential difference, the gate of the FET is only pulled low to the HS pin voltage level and not to the actual source level, which might create issues. For this design, a 1- Ω R_{BOOT} resistor is used in the path of C_{BOOT} and common-mode point, as shown on 图 8.

It is also recommended to place a Schottky diode at the HS pin to further protect the driver from negative spikes.



Copyright © 2017, Texas Instruments Incorporated

图 8. Gate Driver Schematic

2.3.2.3 Gate Drive Resistor

Resistor R_{Gate} is sized to reduce ringing caused by parasitic inductances and capacitances and to limit the current coming out of the gate driver. For this design, a 6- Ω resistor is used for turnon and a 3- Ω resistor for turnoff. Maximum high-side and low-side turnon and turnoff currents are calculated using 公式 4 到 公式 7.

$$I_{HOH} = \frac{V_{DD} - V_{DH} - V_{OH}}{R_{Gate}} = \frac{10\text{ V} - 0.7\text{ V} - 0.45\text{ V}}{6\ \Omega} = 1.475\text{ A} \quad (4)$$

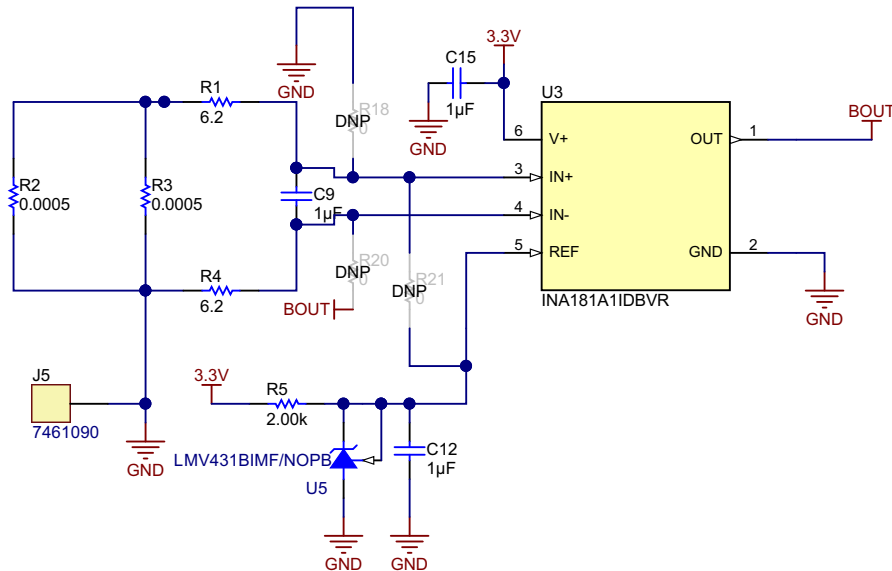
$$I_{LOH} = \frac{V_{DD} - V_{OH}}{R_{Gate}} = \frac{10\text{ V} - 0.45\text{ V}}{6\ \Omega} = 1.592\text{ A} \quad (5)$$

$$I_{HOL} = \frac{V_{DD} - V_{DH} - V_{OL}}{R_{Gate}} = \frac{10\text{ V} - 0.7\text{ V} - 0.25\text{ V}}{3\ \Omega} = 3.02\text{ A} \quad (6)$$

$$I_{LOL} = \frac{V_{DD} - V_{OL}}{R_{Gate}} = \frac{10\text{ V} - 0.25\text{ V}}{3\ \Omega} = 3.25\text{ A} \quad (7)$$

2.3.3 Current Sensing

To protect the FETs from overcurrent failure, a current sensing circuitry is implemented in this design. Usually, an inverter requires to sense both the battery charging and discharging current. Thus, it is necessary to sense current in both directions. This design uses the low-cost bidirectional current sense amplifier INA181 with low-offset voltage, high-gain bandwidth product, and high accuracy, which can be used for high-side and low-side sensing. The current sensing schematic is shown in 图 9.



Copyright © 2017, Texas Instruments Incorporated

图 9. Current Sensing Schematic

The LMV431B is used for shunt reference, which provides a reference voltage of 1.24 V. 公式 8 shows the transfer function of current sensing circuitry.

$$\frac{V_{OUT}}{V_{IN}} = (I_{LOAD} \times R_{SENSE} \times Gain) + V_{REF} \tag{8}$$

To provide flexibility for overall gain, two sense resistors are used in parallel. The TIDA-01292 design uses two 0.5-mΩ resistors in parallel for R_{SENSE} and the INA181 with a fixed gain of 50. This design also uses a low-pass filter with a cutoff frequency of around 13 kHz at the input of the INA181.

A provision to use an op amp and external resistors for adjustment of gain is also provided in this design.

2.3.4 Loss Calculation

Loss calculation is important to theoretically estimate the temperature of various components on the board to estimate the total power handling capability of the design.

The majority of losses that take place in the inverter are the conduction loss, switching loss, body diode conduction loss, loss in the current sense resistor, and loss in the bulk of the PCB.

2.3.4.1 Conduction Loss in MOSFETs

To calculate conduction loss, have the equivalent RMS current through each MOSFET. Due to the nature of the switching technique used, calculating RMS current is not as straight forward as for a normal sine wave.

To calculate the RMS current, the 50-Hz sine wave is divided into two time intervals of 10 ms each. For 10 ms, the top FET is conducting continuously while the bottom FET is off. During this time, conduction loss happens only in the top FET. For the other 10 ms, the top and bottom FETs are switching with sinusoidally varying duty cycle. Note that at any instant, the peak current through the FETs is also varying sinusoidally. Based on 图 4 to 图 7, the current through top and bottom FETs would look something like 图 10 and 图 11, respectively.

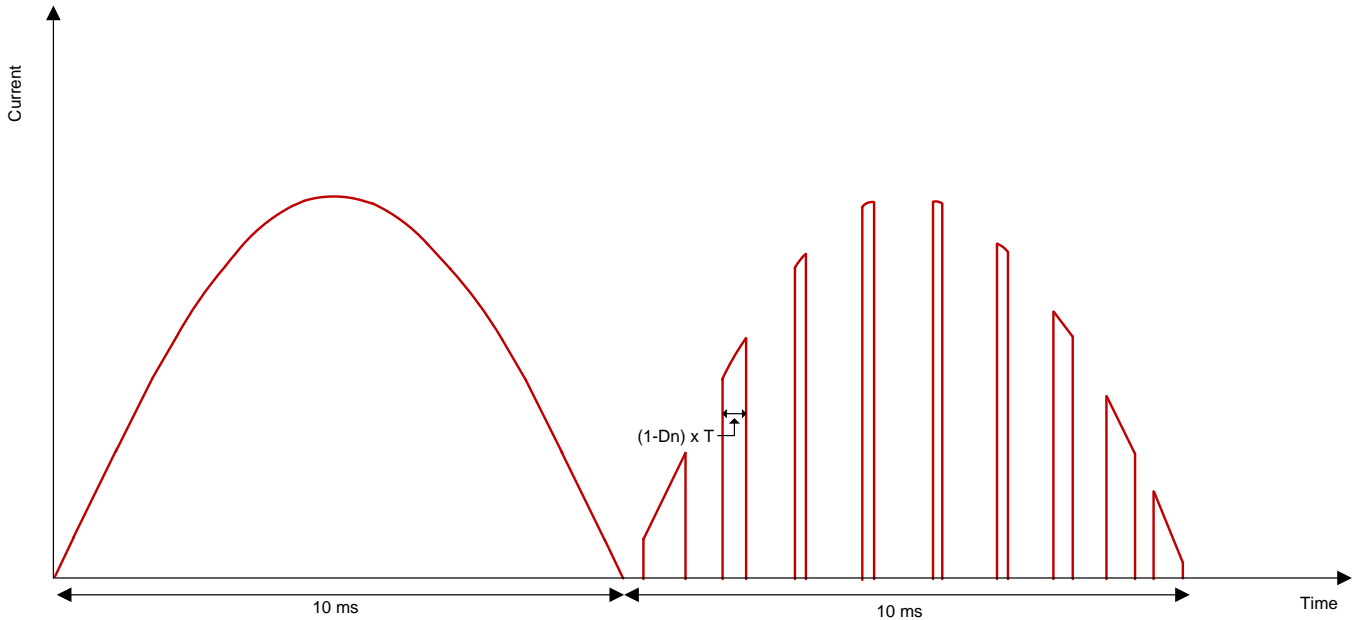


图 10. Current Waveform Through Top FET

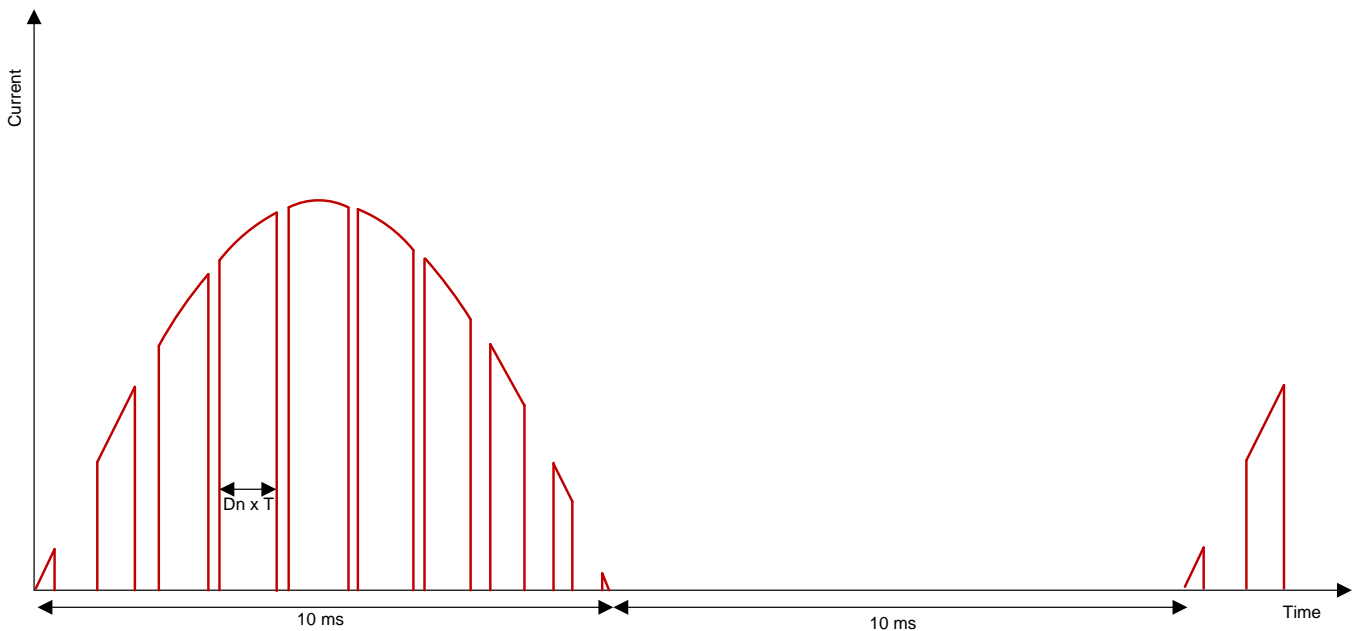


图 11. Current Waveform Through Bottom FET

During the switching period, the total current through the bottom FET is $D_n \times I_{Pn}$ while the current through top FET is $(1 - D_n) \times I_{Pn}$, where D_n is the duty cycle and I_{Pn} is the peak current at that particular switching instant n .

To calculate the total RMS current, the current waveform is divided into two parts of 10 ms each. The RMS current through each FET then would be calculated using 公式 9:

$$I_{RMS} = \sqrt{\frac{(I_{RMS1})^2 + (I_{RMS2})^2}{2}} \quad (9)$$

where:

- I_{RMS1} is the RMS current in the first 10 ms
- I_{RMS2} is the RMS current in the next 10 ms

For the bottom FETs, current flows through them only for 10 ms. To calculate the overall RMS current for the waveform as shown in 图 11, first find out the RMS current for each switching instant given that the duty cycle and peak current for each instant is different and varies sinusoidally. For doing so, all the pulses can be assumed as square pulses because the time period is very small when compared to the 50-Hz sine. For a square pulse of magnitude A , the RMS value is $\sqrt{D} \times A$, where D is the duty cycle of the given pulse. Similarly, the RMS values for the individual pulses shown in 图 11 is $\sqrt{D_n} \times I_{Pn}$, where n is the instant of switching. Total switching instants are calculated using 公式 10:

$$n = \frac{f_{sw}}{50 \text{ Hz}} = \frac{12 \text{ kHz}}{50 \text{ Hz}} = 240 \quad (10)$$

The RMS current through the bottom FET at any instant n is calculated as 公式 11:

$$I_{RMSn_B} = \sqrt{D_n} \times I_P \times \sin\left(\frac{2n\pi}{240}\right) \quad (11)$$

To get sinusoidal output, the duty cycle is also varied in the same fashion. Assuming a modulation index of 1, the duty cycle for n^{th} instant can be calculated using 公式 12. Because the current through the bottom FET flows only for half the time (10 ms), for these calculations, n varies from 0 to 120.

$$D_n = \sin\left(\frac{2n\pi}{240}\right) \quad (12)$$

The total RMS current for this 10 ms is calculated using 公式 13:

$$I_{RMS1_B} = \sqrt{\frac{\sum_{n=1}^{120} I_{RMSn_B}^2}{120}} \quad (13)$$

Therefore, the RMS current for bottom FET I_{RMS_B} is calculated using 公式 14:

$$I_{RMS_B} = \sqrt{\frac{(I_{RMS1_B})^2 + (I_{RMS2_B})^2}{2}} = \sqrt{\frac{\left(\sqrt{\frac{\sum_{n=1}^{120} I_{RMSn_B}^2}{120}}\right)^2 + (0)^2}{2}} = \sqrt{\frac{\sum_{n=1}^{120} I_{RMSn_B}^2}{120 \times 2}} \quad (14)$$

I_{RMS2} for the bottom FET is zero because one of the bottom FETs is continuously off for 10 ms.

Calculating the RMS current for the top FET is similar to the bottom FET. The only difference is that the conduction time for the top FET is $(1 - D_n)$ for I_{RMS1} , ignoring the dead time, and I_{RMS2} is not zero but a sine output. Again approximating the pulses to be square, the I_{RMSn} for n^{th} switching instant for the top FET can be calculated using 公式 15:

$$I_{RMSn_T} = \sqrt{(1 - D_n)} \times I_p \times \sin\left(\frac{2n\pi}{240}\right) \quad (15)$$

Calculating D_n remains same as given by 公式 12. The RMS current for the switching time, I_{RMS1} , for the top FET is calculated using 公式 16:

$$I_{RMS1_T} = \sqrt{\frac{\sum_{n=1}^{120} I_{RMSn_T}^2}{120}} \quad (16)$$

The total RMS current for top FET is thus calculated using 公式 17:

$$I_{RMS_T} = \sqrt{\frac{(I_{RMS1_T})^2 + (I_{RMS2_T})^2}{2}} = \sqrt{\frac{\left(\sqrt{\frac{\sum_{n=1}^{120} I_{RMSn_T}^2}{120}}\right)^2 + \left(\frac{I_p}{\sqrt{2}}\right)^2}{2}} = \sqrt{\frac{\frac{\sum_{n=1}^{120} I_{RMSn_T}^2}{120} + \left(\frac{I_p}{\sqrt{2}}\right)^2}{2}} \quad (17)$$

2.3.4.2 Switching Loss

One calculates the total switching loss usually by multiplying the energy lost and frequency to get the power loss. But in this case, because the peak current at every switching instant is different, the energy transferred at each instant is also different. Thus, to find out the total switching power loss, add up the energy transferred at each instant and find its average over the 50-Hz cycle.

The average of 公式 4 and 公式 5 gives the average turnon current (I_{Turnon}), and the average of 公式 6 and 公式 7 gives the average turnoff current ($I_{Turnoff}$). Because a 2-A driver is used for this design, the upper limit on the source and sink current is 2 A.

The energy transferred during the n^{th} turnon and turnoff instant is calculated using 公式 18 and 公式 19, respectively:

$$E_{Turnon_n} = \frac{1}{2} \times V_{DS} \times I_n \times \frac{(Q_{gs} - Q_{gs(th)} + Q_{gd})}{I_{Turnon}} \quad (18)$$

$$E_{Turnoff_n} = \frac{1}{2} \times V_{DS} \times I_n \times \frac{(Q_{gs} - Q_{gs(th)} + Q_{gd})}{I_{Turnoff}} \quad (19)$$

where:

- V_{DS} is the drain-source voltage across FET
- I_n is the current at n^{th} switching instant and is given by 公式 20
- Q_{gs} is the total gate-source charge of the MOSFET, 17.1 nC for the CSD17573Q5B FET
- $Q_{gs(th)}$ is the gate-source charge at the threshold voltage, 8.6 nC for the CSD17573Q5B
- Q_{gd} is the gate-drain charge of the MOSFET, 11.9 nC for the CSD17573Q5B

$$I_n = I_p \times \sin\left(\frac{2n\pi}{240}\right) \quad (20)$$

The total power loss at turnon and turnoff is calculated using 公式 21 and 公式 22:

$$P_{\text{loss_on}} = \frac{\sum_{n=1}^{120} E_{\text{Turnon}_n}}{20 \text{ ms}} \quad (21)$$

$$P_{\text{loss_off}} = \frac{\sum_{n=1}^{120} E_{\text{Turnoff}_n}}{20 \text{ ms}} \quad (22)$$

Note that any of the four MOSFETs switches, only for half the cycle (10 ms)—thus only 120 energy instants—are added up to calculate power loss. Due to the switching scheme used, the top FET is always soft switching. As a result, the majority of switching losses are in the bottom FETs only. To calculate the switching loss across top FET accurately, replace V_{DS} with the forward drop of the body diode of the FET.

2.3.4.3 Body Diode Loss

To ensure there is not any shoot-through condition, a dead time of 500 ns is provided in the firmware. During this dead time, the entire load current flows through the body diode, causing power loss across it. Because the dead time appears twice during one switching cycle, that is at turnon and turnoff, consider it twice at all switching instants. Again, because the peak current flowing through it varies sinusoidally, calculate the energy at all these instants, add them up, and find the average over one entire cycle of 50 Hz. The energy at any instant n is calculated using 公式 23:

$$E_{n_body_diode} = 2 \times V_f \times I_n \times t_d \quad (23)$$

where:

- V_f is the forward voltage drop of the body diode
- I_n is the current at n^{th} instant given by 公式 20
- t_d is the dead time (500 ns for this design)

The total power loss in one leg is thus calculated using 公式 24:

$$P_{\text{body_diode}} = \frac{\sum_{n=1}^{120} E_{n_body_diode}}{20 \text{ ms}} \quad (24)$$

Body diode loss occurs only in the top MOSFETs for the PWMs used for this design because bottom switches are hard switched every time.

2.3.4.4 Miscellaneous Losses

In addition to the major losses mentioned previously:

- Board copper: This loss depends on board dimension, Cu thickness, and FET placement. There is also a considerable amount of conduction losses in the board copper as well.
- Input bulk capacitors: The electrolytic capacitors present at the input also result in conduction loss depending on the ripple current and the ESR of the capacitor.
- Sense resistor: Because the load current for this design is large, there is conduction loss in sense resistor as well, which cannot be ignored.
- Other than these components, there is also power loss in the gate drivers and LDOs, but this is usually

very small compared to other losses and thus can be ignored.

3 Hardware, Testing Requirements, and Test Results

3.1 Hardware

图 12 shows the test setup of the board with the transformer, bulb loads, and interface to the TMS320F28027 LaunchPad for firmware.

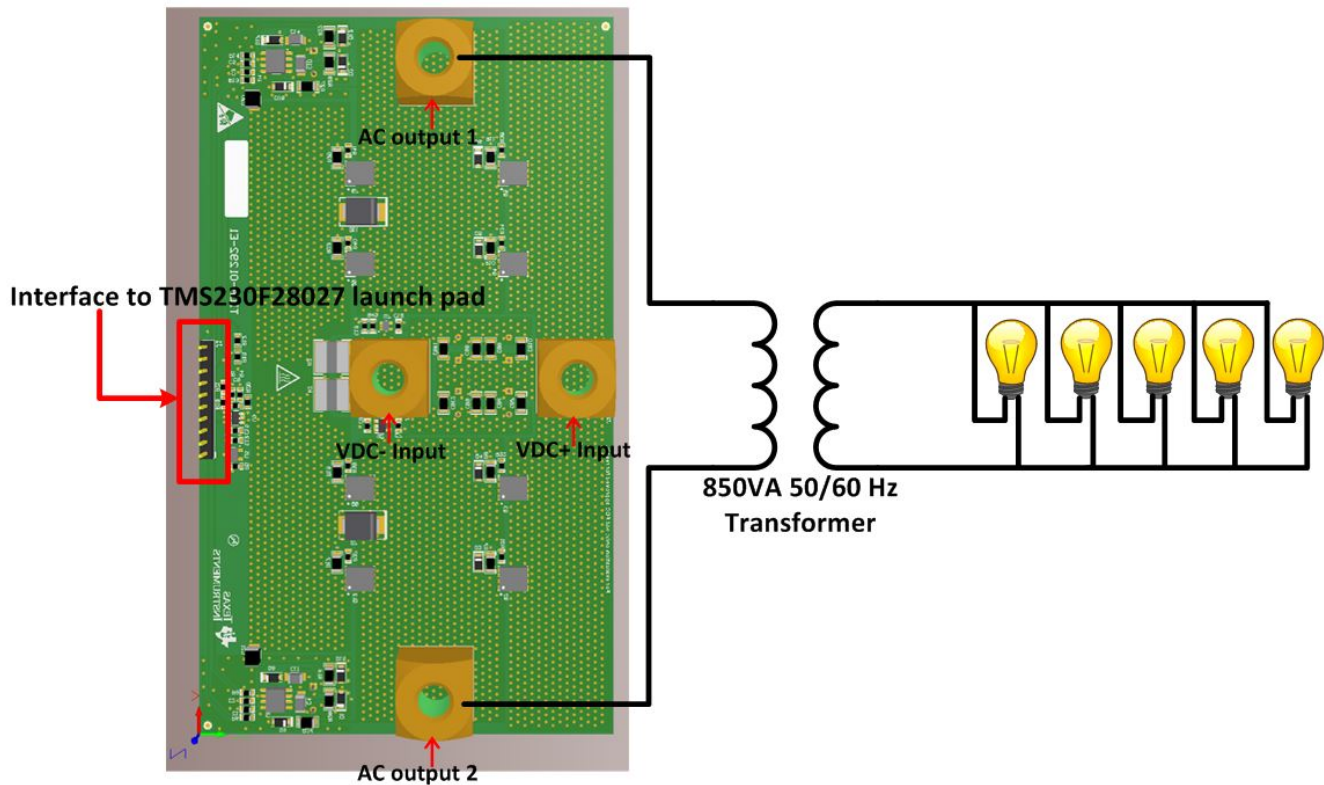


图 12. TIDA-01292 Test Setup

The details of the interface to the LaunchPad, connector J1 are as follows:

- Pin 1: Gate input for the high-side FET of left leg
- Pin 2: Gate input for the low-side FET of left leg
- Pin 3, 6, 7: Ground reference
- Pin 4: Analog output of current sense amplifier
- Pin 5: VDC sense output
- Pin 8: Temperature sense output
- Pin 9: Gate input for the high-side FET of right leg
- Pin 10: Gate input for the low-side FET of the right leg

3.2 Testing and Results

The TIDA-01292 design is tested with bulb loads and a 850-VA, 50-Hz transformer at the output.

3.2.1 Efficiency

The efficiency of the design is tested at various FAN speeds. 表 2, 表 3, and 表 4 show the efficiency of the design at 800-LFM, 600-LFM, and 400-LFM fan speeds with a 12-V battery input. The efficiency figures are for the TIDA-01292 board only and do not include the losses in the transformer.

表 2. Efficiency With 12-V Battery Input and 800-LFM Fan Speed

V_{IN_RMS} (V)	I_{IN_RMS} (A)	P_{IN} (W)	V_{OUT_RMS} (V)	I_{OUT_RMS} (A)	P_{OUT} (W)	EFFICIENCY
11.88	14.58	139.54	9.03	21.04	138.66	99.37%
11.83	26.43	250.07	8.88	33.30	246.88	98.72%
11.78	38.30	357.56	8.73	46.93	350.11	97.92%
11.73	49.50	456.03	8.59	60.18	442.76	97.09%
11.71	55.02	504.55	8.51	66.90	487.51	96.62%
11.68	60.42	550.85	8.44	73.45	529.71	96.16%
11.66	65.52	594.07	8.37	79.73	568.84	95.75%
11.64	70.44	635.16	8.30	85.89	606.28	95.45%
11.63	72.85	655.61	8.27	88.85	623.86	95.16%
11.62	75.13	674.30	8.24	91.70	640.38	94.97%

表 3. Efficiency With 12-V Battery Input and 600-LFM Fan Speed

V_{IN_RMS} (V)	I_{IN_RMS} (A)	P_{IN} (W)	V_{OUT_RMS} (V)	I_{OUT_RMS} (A)	P_{OUT} (W)	EFFICIENCY
11.94	4.14	21.37	9.22	15.14	21.31	99.72%
11.88	14.57	139.30	9.03	21.07	138.54	99.45%
11.83	26.42	249.88	8.88	33.29	246.56	98.67%
11.77	38.24	356.95	8.73	46.85	349.35	97.87%
11.73	49.42	455.98	8.59	60.12	442.26	96.99%
11.71	54.97	504.10	8.51	66.81	486.86	96.58%
11.68	60.33	550.21	8.44	73.36	529.13	96.17%
11.66	65.45	593.32	8.37	79.72	568.74	95.86%
11.64	70.38	634.89	8.30	85.77	605.15	95.32%
11.63	72.67	653.64	8.26	88.68	621.73	95.12%
11.62	74.91	671.90	8.23	91.47	638.22	94.99%

表 4. Efficiency With 12-V Battery Input and 400-LFM Fan Speed

V_{IN_RMS} (V)	I_{IN_RMS} (A)	P_{IN} (W)	V_{OUT_RMS} (V)	I_{OUT_RMS} (A)	P_{OUT} (W)	EFFICIENCY
11.88	14.56	139.07	9.03	21.10	138.43	99.54%
11.83	26.39	249.67	8.88	33.27	246.21	98.61%
11.78	38.21	356.72	8.73	46.82	349.14	97.88%
11.73	49.36	455.35	8.59	60.02	441.45	96.95%
11.70	54.93	503.56	8.51	66.79	486.64	96.64%
11.68	60.23	549.20	8.44	73.26	528.42	96.22%
11.66	65.28	591.93	8.37	79.49	567.01	95.79%
11.64	70.30	634.54	8.30	85.61	604.31	95.24%
11.63	72.60	653.54	8.27	88.50	621.06	95.03%
11.62	74.87	672.21	8.23	91.33	637.45	94.83%

The design was also tested for efficiency at 10-V and 14-V battery inputs at a 600-LFM fan speed. 表 5 和 表 6 显示 10-V 和 14-V 电池输入的数据，分别。

表 5. Efficiency With 10-V Battery Input and 600-LFM Fan Speed

V _{IN_RMS} (V)	I _{IN_RMS} (A)	P _{IN} (W)	V _{OUT_RMS} (V)	I _{OUT_RMS} (A)	P _{OUT} (W)	EFFICIENCY
10.06	2.03	13.74	7.78	6.77	14.30	104.05%
10.01	12.94	105.20	7.61	16.31	104.79	99.61%
9.96	23.84	190.11	7.47	28.90	187.55	98.65%
9.91	34.60	271.78	7.33	41.78	265.68	97.76%
9.87	44.65	346.19	7.20	54.05	335.75	96.98%
9.83	54.28	415.84	7.08	65.86	399.48	96.07%
9.81	58.54	445.90	7.02	71.18	426.65	95.68%
9.79	62.81	476.23	6.96	76.40	452.83	95.09%
9.78	66.72	503.00	6.90	81.36	476.59	94.75%
9.76	70.59	529.58	6.85	86.25	499.96	94.40%
9.74	75.15	560.71	6.79	91.95	525.88	93.79%
9.73	78.63	584.16	6.74	96.38	545.06	93.31%

表 6. Efficiency With 14-V Battery Input and 600-LFM Fan Speed

V _{IN_RMS} (V)	I _{IN_RMS} (A)	P _{IN} (W)	V _{OUT_RMS} (V)	I _{OUT_RMS} (A)	P _{OUT} (W)	EFFICIENCY
13.91	10.06	43.62	10.92	41.55	37.66	86.34%
13.83	17.07	182.85	10.48	34.48	179.27	98.04%
13.76	29.37	320.80	10.33	42.63	315.12	98.23%
13.72	42.07	456.39	10.18	54.67	445.75	97.67%
13.69	48.94	527.83	10.09	61.99	513.55	97.29%
13.65	55.50	595.23	10.00	69.28	576.93	96.93%
13.63	61.78	658.97	9.92	76.51	636.25	96.55%
13.60	67.94	720.42	9.83	83.69	692.64	96.14%
13.58	73.77	778.77	9.75	90.58	744.19	95.56%

3.2.2 Functional Waveforms

图 13 和 图 14 显示高边和低边 FET 的栅极-源极和漏极-源极波形，分别用于底部 FET 的开通和关断。

注：
 Channel 1 (Yellow): VDS_LS—低边 FET 的漏极-源极波形，10 V/div
 Channel 2 (Green): VGS_LS—低边 FET 的栅极-源极波形，10 V/div
 Channel 3 (Purple): VGS_HS—高边 FET 的栅极-源极波形，10 V/div
 Time scale: 200 ns/div

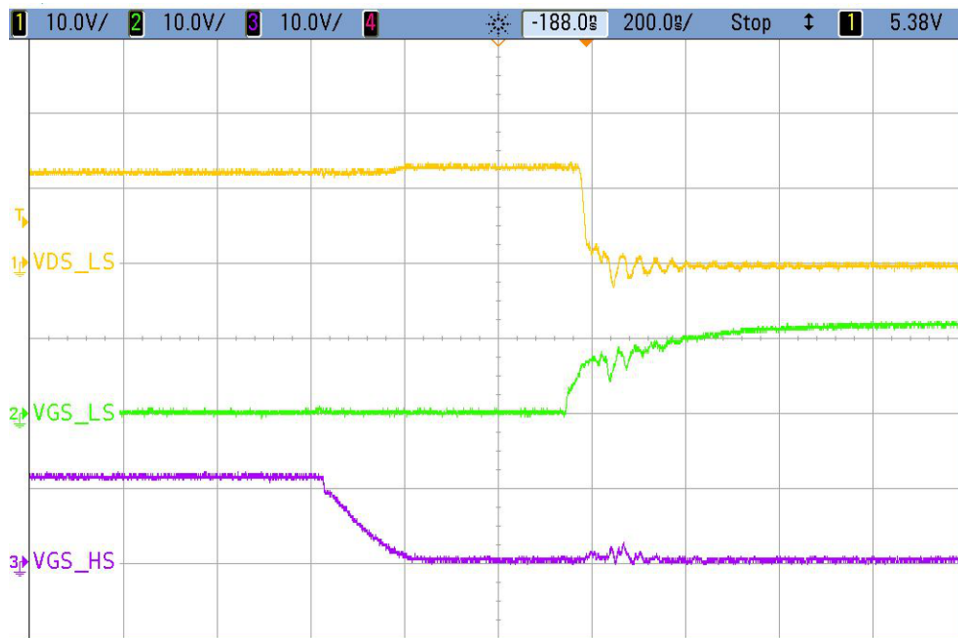


图 13. Switching Waveform for Turnon of Bottom FETs

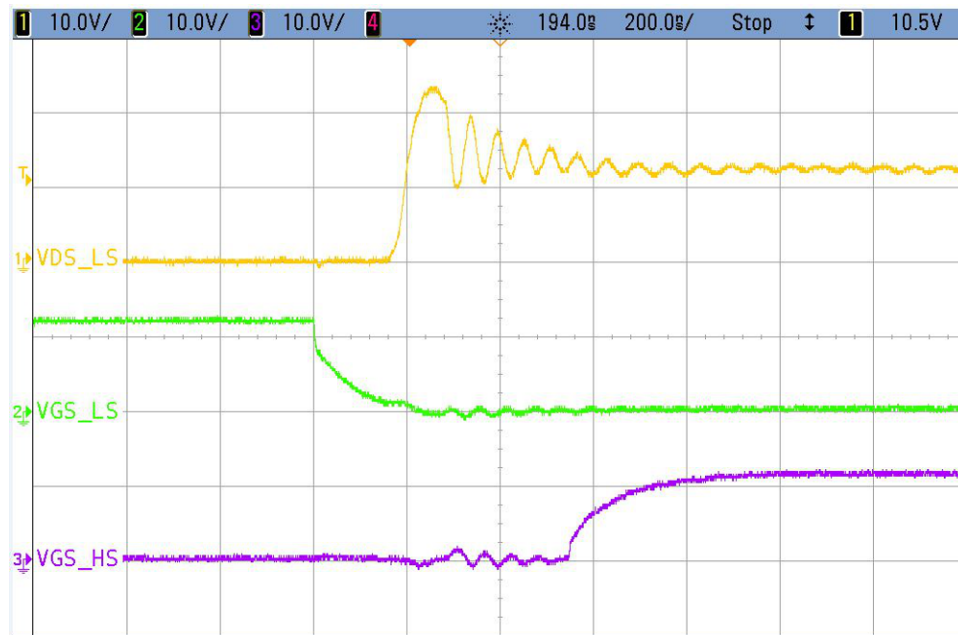


图 14. Switching Waveform for Turnoff of Bottom FETs

The TIDA-01292 design has a dead time of about 350 ns existing between the top and bottom FETs.

This design was also tested for inductive load where the primary winding of an auto-transformer was used as the inductive load. 图 15 shows the filtered voltage and current output for the inductive load.

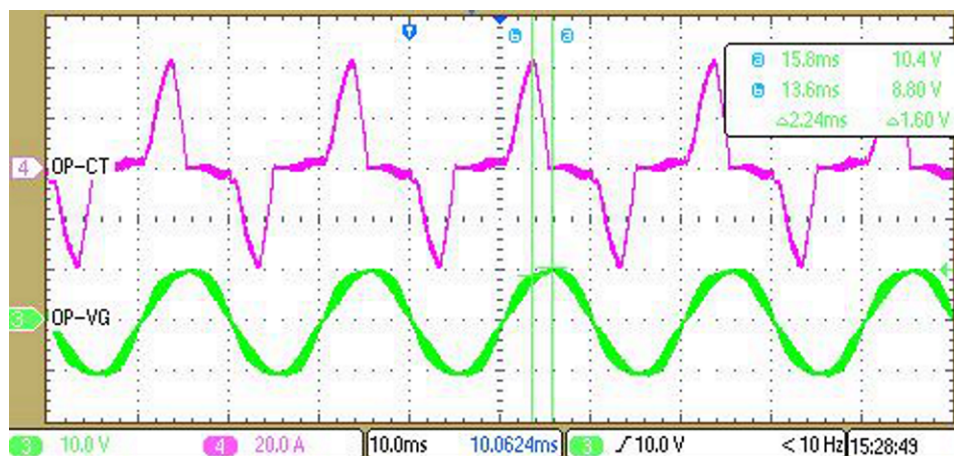


图 15. Output Waveform for Inductive Load

To further protect the FETs, this design has an overload and overcurrent protection algorithm where if the current hits the assigned peak, the PWMs shut off for 2 ms before starting again. 图 16 和 图 17 显示该情况下的响应。

注: Channel 2 (Purple): 220-V AC output voltage, 500 V/div
 Channel 3 (Green) : Output of INA181, 2 V/div
 Channel 4 (Teal): Output current, 100 A/div

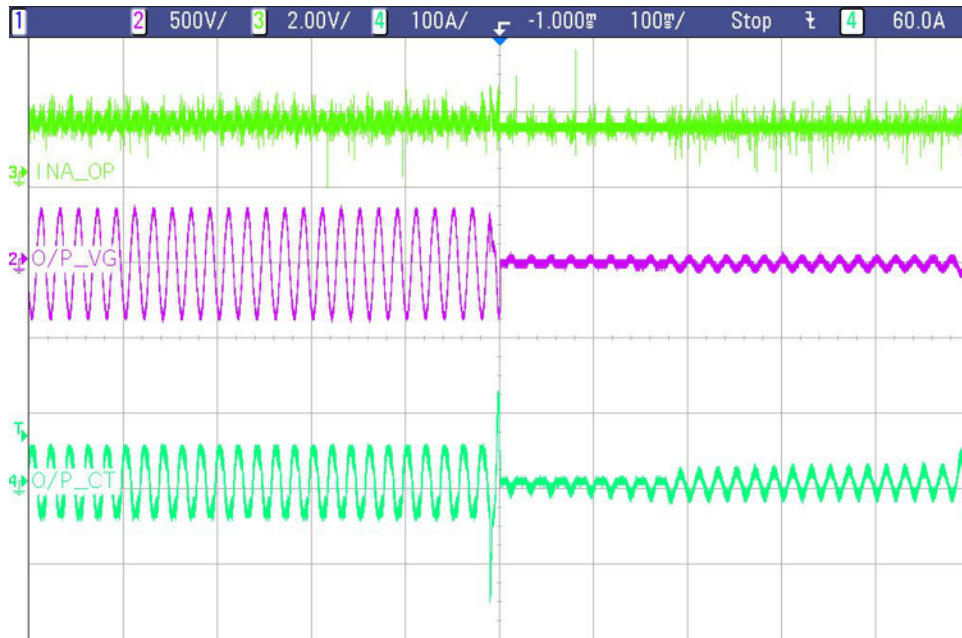


图 16. Overcurrent Protection

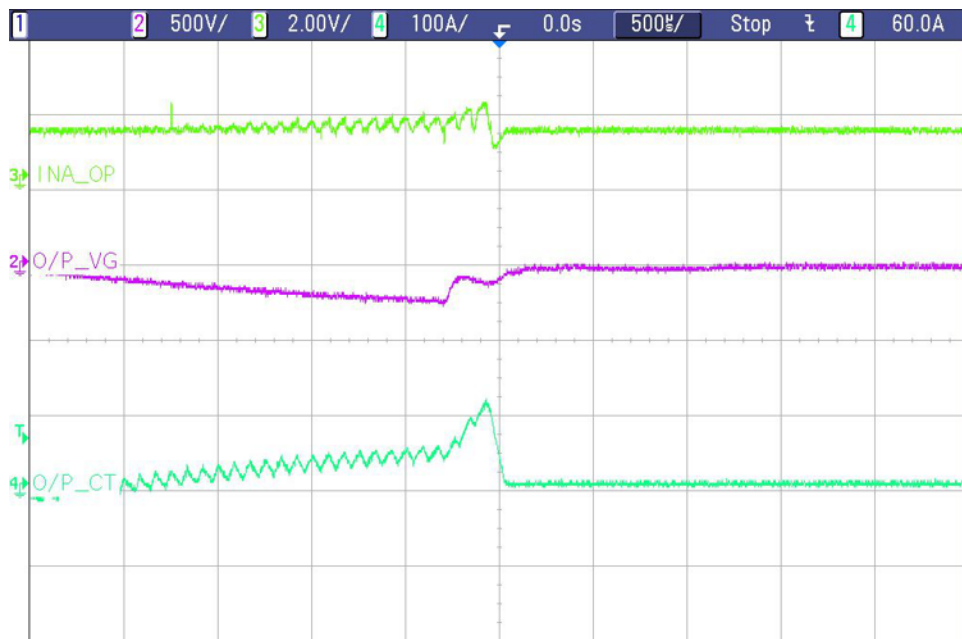


图 17. Overcurrent Protection (Zoomed)

3.2.3 Thermal Performance

图 18 shows the thermal performance of the design at full load, 12-V battery input, and 400-LFM fan speed.

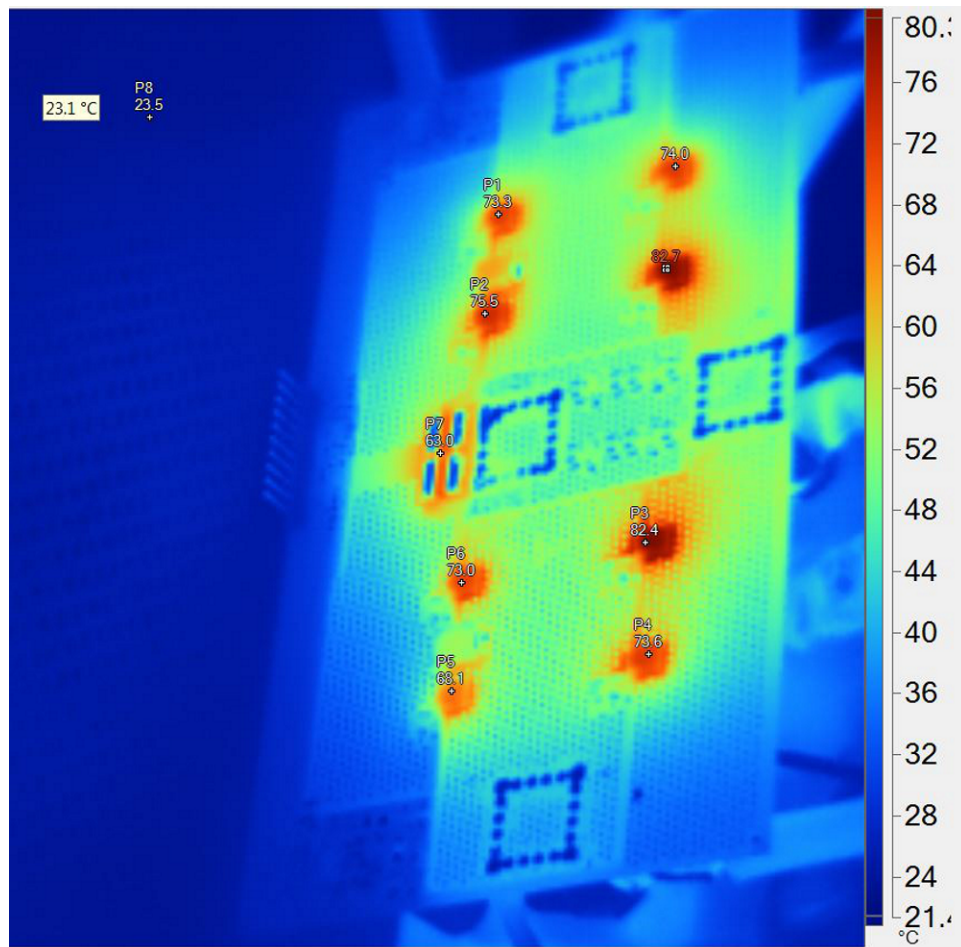


图 18. Thermal Image at Full Load, 12-V Battery Input, and 400-LFM Fan Speed

4 Design Files

4.1 Schematics

To download the schematics, see the design files at [TIDA-01292](#).

4.2 Bill of Materials

To download the bill of materials (BOM), see the design files at [TIDA-01292](#).

4.3 PCB Layout Recommendations

The optimum performance of high- and low-side gate drivers cannot be achieved without taking due considerations during the circuit board layout. Consider the following during the board layout:

- Connect low-ESR or ESL capacitors close to the device, between VDD and VSS pins to support the high-peak currents being drawn from VDD during turnon of the external MOSFET.
- Connect a low-ESR electrolytic capacitor between MOSFET drain and ground (VSS) to prevent large voltage transients at the drain of the top MOSFET.
- Minimize the parasitic inductances in the source of top MOSFET and in the drain of the bottom MOSFET to avoid large negative transients on the switch node (HS pin).
- Grounding considerations:
 1. The first priority in designing grounding connections is to confine the high-peak currents that charge and discharge the MOSFET gate into a minimal physical area. This current decreases the loop inductance and minimizes noise issues on the gate terminal of the MOSFET. Place the MOSFETs as close as possible to the gate driver.
 2. The second high-current path includes the bootstrap capacitor, the bootstrap diode, the local ground referenced bypass capacitor, and low-side MOSFET body diode. The bootstrap capacitor is recharged on a cycle-by-cycle basis through the bootstrap diode from the ground referenced VDD bypass capacitor. The recharging occurs in a short time interval and involves high peak current. Minimize this loop length and area on the circuit board to ensure reliable operation.

4.3.1 Layout Prints

To download the layer plots, see the design files at [TIDA-01292](#).

4.4 Altium Project

To download the Altium project files, see the design files at [TIDA-01292](#).

4.5 Gerber Files

To download the Gerber files, see the design files at [TIDA-01292](#).

4.6 Assembly Drawings

To download the assembly drawings, see the design files at [TIDA-01292](#).

5 Software Files

To download the software files, see the design files at [TIDA-01292](#).

6 Related Documentation

1. Texas Instruments, [AN-2296 SM72295: Highly Integrated Gate Driver for 800VA to 3KVA Inverter](#), Application Report (SNVA678)
2. Texas Instruments, [800VA Pure Sine Wave Inverter's Reference Design](#), Application Report (SLAA602)

6.1 商标

Piccolo, LaunchPad are trademarks of Texas Instruments.
All other trademarks are the property of their respective owners.

7 About the Authors

NEHA NAIN is a systems engineer at Texas Instruments, where she is responsible for developing reference design solutions for the power delivery, industrial segment. Neha earned her bachelor in electrical and electronics engineering from the PES Institute of Technology (now PES University), Bangalore.

SHREENIDHI PATIL is an analog application engineer at Texas Instruments, where he is responsible for supporting various customers in North India. Shreenidhi earned his bachelor in electrical and electronics engineering from the RV College of Engineering, Bangalore.

7.1 Acknowledgments

Special thanks to **VIKAS CHOLA**, Field Applications Engineer, for his invaluable assistance in helping with the firmware and implementing various protections while testing this design.

修订历史记录

注：之前版本的页码可能与当前版本有所不同。

Changes from A Revision (February 2018) to B Revision **Page**

- 已添加 *INA185*..... 8
-

Changes from Original (September 2017) to A Revision **Page**

- Omitted note for [公式 14](#)..... 16
-

重要声明和免责声明

TI“按原样”提供技术和可靠性数据（包括数据表）、设计资源（包括参考设计）、应用或其他设计建议、网络工具、安全信息和其他资源，不保证没有瑕疵且不做任何明示或暗示的担保，包括但不限于对适销性、某特定用途方面的适用性或不侵犯任何第三方知识产权的暗示担保。

这些资源可供使用 TI 产品进行设计的熟练开发人员使用。您将自行承担以下全部责任：(1) 针对您的应用选择合适的 TI 产品，(2) 设计、验证并测试您的应用，(3) 确保您的应用满足相应标准以及任何其他功能安全、信息安全、监管或其他要求。

这些资源如有变更，恕不另行通知。TI 授权您仅可将这些资源用于研发本资源所述的 TI 产品的应用。严禁对这些资源进行其他复制或展示。您无权使用任何其他 TI 知识产权或任何第三方知识产权。您应全额赔偿因在这些资源的使用中对 TI 及其代表造成的任何索赔、损害、成本、损失和债务，TI 对此概不负责。

TI 提供的产品受 [TI 的销售条款](#) 或 [ti.com](#) 上其他适用条款/TI 产品随附的其他适用条款的约束。TI 提供这些资源并不会扩展或以其他方式更改 TI 针对 TI 产品发布的适用的担保或担保免责声明。

TI 反对并拒绝您可能提出的任何其他或不同的条款。

邮寄地址：Texas Instruments, Post Office Box 655303, Dallas, Texas 75265

Copyright © 2022，德州仪器 (TI) 公司